

Diglycolamide functionalized multi-walled carbon nanotubes for removal of uranium from aqueous solution by adsorption

Ashish Kumar Singha Deb · P. Ilaiyaraja ·
D. Ponraju · B. Venkatraman

Received: 12 July 2011 / Published online: 11 August 2011
© Akadémiai Kiadó, Budapest, Hungary 2011

Abstract Diglycolamide functionalized multi-walled carbon nanotubes (DGA-MWCNTs) were synthesized by sequential chemical reactions for removal of uranium from aqueous solution. Characterization studies were carried out using FT-IR spectroscopy, XRD and SEM analysis. Adsorption of uranium from aqueous solution on this material was studied as a function of nitric acid concentration, adsorbent dose and initial uranium concentration. The uranium adsorption data on DGA-MWCNTs followed the Langmuir and Freundlich adsorption isotherms. The adsorption capacity of DGA-MWCNTs as well as adsorption isotherms and the effect of temperature on uranium ion adsorption were investigated. The standard enthalpy, entropy, and free energy of adsorption of the uranium with DGA-MWCNTs were calculated to be $6.09 \text{ kJ mole}^{-1}$, $0.106 \text{ kJ mole}^{-1} \text{ K}^{-1}$ and $-25.51 \text{ kJ mole}^{-1}$ respectively at 298K. The results suggest that DGA-MWCNTs can be used as efficient adsorbent for uranium ion removal.

Keywords Multiwalled carbon nanotubes · Functionalization · Uranium · Adsorption · Adsorption isotherm · Free energy of adsorption

Introduction

Since the discovery of carbon nanotubes (CNTs) in 1991 [1], scientists and technologists have welcomed this cylindrical allotrope of carbon as one of the most researched material world-wide. CNTs exhibit unique physical and chemical properties. CNTs include single-walled (SWCNTs) and multi-walled (MWCNTs) depending on the number of layers comprising them. Due to porous and hollow structures, large surface area, low density, high mechanical, thermal and chemical stabilities, CNTs possess great potential as an adsorbent for removing a wide variety of organic compounds and metals ions from aqueous or organic medium. Examples include: organic compounds such as dioxin [2], resorcinol and other phenolic derivatives [3], thiophene [4], fulvic acid [5], trihalomethanes [6], chlorinated aliphatic and aromatic compounds [7], phenolic compounds [8], dyes [9], pesticides [10] etc. and metal ions such as lead, copper, cadmium [11], iron [12] zinc [13], nickel [14], chromium [15], cobalt, manganese [16] strontium [17], silver [18]. It has been used for removal of contaminants in drinking water [19]. Recently CNTs have been applied for recovery of radionuclide such as thorium [20], europium [21], americium [22], uranium [23] and plutonium [24] from aqueous solution.

In all the above applications, CNTs were used in pristine form. For optimum selective performances towards specific metal ions or organic molecules CNTs need to be modified without much alternation of their physical and chemical properties. Modification of CNTs can be accomplished through covalent functionalization and non-covalent functionalizations [25]. Organic covalent functionalization of CNTs have been employed [26] and functionalized CNTs were used for adsorbent application. Carboxy functionalized multi-walled CNTs used for adsorption of zinc [27]

A. K. S. Deb (✉) · P. Ilaiyaraja · B. Venkatraman
Radiological Safety Division, Radiological Safety
and Environmental Group, Indira Gandhi Centre for Atomic
Research, Kalpakkam 603102, Tamilnadu, India
e-mail: ashishk@igcar.gov.in

D. Ponraju
Safety Engineering Division, Indira Gandhi Centre for Atomic
Research, Kalpakkam 603102, Tamilnadu, India

and azo dye [28] from aqueous solution. Hexahistidine-tagged protein functionalized MWCNTs have been used for selective adsorption of copper and nickel from aqueous solution [29]. MWCNTs functionalized with 1-(2-pyridylazo)-2-naphthol have been used for adsorption of trace amounts of cobalt ion in aqueous solution [30]. Modification of MWCNTs not only enhances the adsorption but also fastens the kinetics of adsorption [27, 29]. According to surface complexation model [23] it is most plausible that these adsorption reactions proceed at specific surface sites/functional groups.

Extraction and pre-concentration of valuable actinide metal ions from aqueous solution are extremely important not only for limited resource availability, but also to reduce their quantum for disposal as radioactive wastes [31]. Various ligands such as phosphates, diglycolamide (DGA) derivatives, malonamides and triazine derivatives are being employed for this purpose. Among the ligands, diglycolamides is a tridentate ligand due to which it possesses greater tendency to bind with metal ions. They are also related to the harmless nature of their degradation products and to the possibility to incinerate the used solvents leading to minimization of the volume of secondary waste. DGA derivatives such as *N,N,N',N'*-tetraoctyldiglycolamide (TODGA) and *N,N,N',N'*-tetrakis-2-ethylhexyldiglycolamide (TEHDGA) have been applied for the separation of uranium in aqueous solution [32–36].

In this study, multi-walled CNTs are modified with diglycolamide groups by sequential chemical reaction and this functionalized multi-walled CNTs (DGA-MWCNT) have been used for the separation of uranium from aqueous solution. Studies such as the effect of nitric acid concentration, initial uranium concentration, DGA-MWCNTs dose and temperature on adsorption performance have been carried out. The adsorption isotherms were analyzed in terms of Langmuir and Freundlich equations and the thermodynamic constants (ΔH° , ΔS° and ΔG°) were evaluated.

Experimental

Materials and methods

All chemicals were of analytical reagent grade and used without any further purification. MWCNTs, obtained by chemical vapour deposition method. Characteristics of the MWCNTs are given in Table 1.

Millipore water (resistivity 18.2 m Ω .cm) was used in all experiments. KS 4000i control-incubator shaker (IKA make) was used for equilibration studies. Echo Testr pH2 (Eutech make) pH meter was used for pH adjustment.

Table 1 Characteristics of MWCNTs

Purity	>95 vol%
Amorphous carbon	<2%
Ash	<0.2 wt%
Diameter	10–30 nm
Length	1–2 μ m
Specific surface area	300–600 m ² /g

Millipore vacuum filtration unit with 0.22 μ m Millipore membrane filter was used for filtration. Refrigerated centrifuge (REMI Model No. C-24 BL) was used for separation of CNTs from aqueous/organic solution. Vacuum oven (SEMCO make) and Ultrasonic bath (Life-care make EN 50US) were employed during experiment.

Functionalization of MWCNTs

MWCNTs were subjected to sequential chemical functionalization to prepare diglycolamide functionalized multi-walled CNTs. The functionalization involves carboxylation, acylation, amidation and diglycolamide functionalization. The work flow sheet of sequential functionalization of MWCNTs is given in Scheme 1.

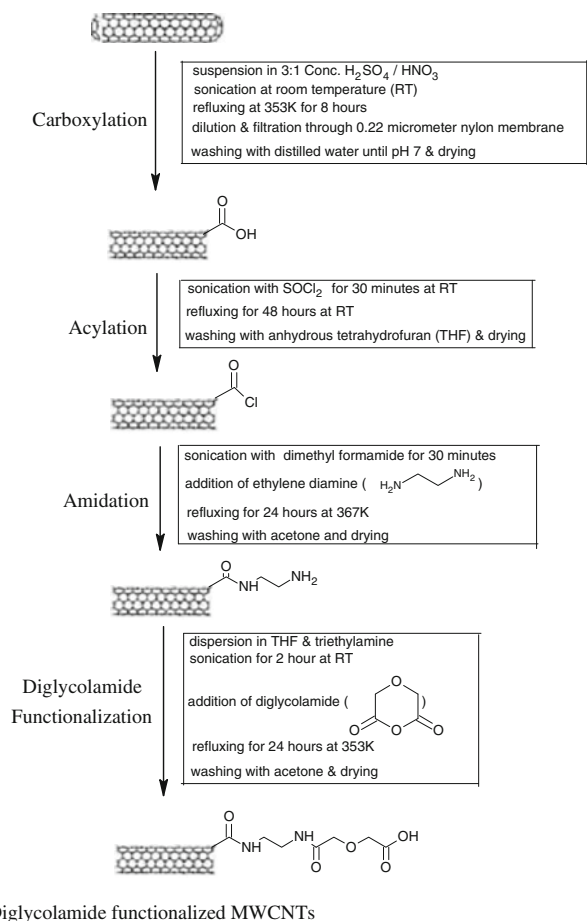
Characterization of functionalized MWCNTs

The MWCNTs and functionalized MWCNTs were characterized by Fourier transform-infrared (FTIR) spectroscopy, X-ray diffraction analysis (XRD) and scanning electron microscopy (SEM). The sample of the FTIR measurement was mounted on a MB 3000 spectrometer (ABB) in KBr pellet at room temperature. The XRD characterization was performed by using X-ray diffraction with Cu K α radiation at room temperature using a STOE diffractometer operated in Bragg-Brentano geometry and attached with a secondary graphite monochromator. The measurements were performed over the angular range $2\theta = 30^\circ$ – 96° in steps of 0.05° . The morphology of the pristine and functionalized MWCNTs was examined by using a field emission scanning electron microscopy.

Uranium adsorption studies

Uranium separation studies were carried out at room temperature. In all experiments, polypropylene centrifuge tubes with screw lids were used in order to prevent radionuclide sorption on the walls of the tubes. Exactly 5 mg of DGA-MWCNTs was taken in a 50 mL centrifuge tube and suitable concentration of uranium was maintained

Multi walled carbon nanotubes (MWCNTs)

**Scheme 1** Flow sheet of chemical modifications on MWCNTs

by adding appropriate volume of aqueous solution of uranyl nitrate stock solution (100 mg L^{-1}). Dilute nitric acid was added to maintain desired acid concentration. 10 mL of above mixture in a 50 mL centrifuge tube was shaken mechanically for equilibration using an orbital shaker at room temperature for 3 h. The suspended solution then centrifuged at 5,000 rpm. Exactly 1 mL of supernatant aliquot was subsequently withdrawn and concentration of uranium was measured by fluorescence spectrometry. The sample was diluted with a 10 wt% phosphoric acid (H_3PO_4) solution. The complex formation of uranium with H_3PO_4 causes a large enhancement of their fluorescence emission intensity. This provides the basis of a uranium assay method with a detection limit of ~ 40 ppb [37]. A calibration graph was plotted by measuring the intensity of fluorescence emission spectra for various concentrations of uranium in 10 wt% H_3PO_4 solution. All fluorescence emission spectra were recorded by a Jobin Yvow-spex Fluorolog spectrofluorimeter using excitation wave length 323 nm. The emission spectra were taken between 450 and

550 nm with 3 nm slit width. The intensity of the emission peak at ~ 493 nm was used to draw the calibration curve as well as to determine the uranium concentration.

The percentage of adsorption (S) was calculated as

$$S = \frac{C_o - C_e}{C_o} \times 100 \quad (1)$$

where, C_o (mg L^{-1}) is the initial concentration of uranium and C_e (mg L^{-1}) is the concentration of uranium in supernatant after equilibrium.

The distribution coefficient (K_d) was calculated as

$$K_d = \frac{C_o - C_e}{C_e} \times \frac{V}{m} \quad (2)$$

where, V (mL) is the volume of the solution and m (g) is the amount of adsorbent.

The above experiments were repeated with various nitric acid concentrations (0.1 to 8 M) to study the effect of acid concentration on adsorption of uranium in DGA-MWCNTs. Experiments were also repeated with various uranium concentrations (2 to 20 mg/L) to study the effect of uranium concentration. All these experiments were carried out with constant amount of DGA-MWCNTs (5 mg). Similarly, the effect of adsorbent dose was studied with fixed uranium concentration (20 mg/mL) by varying the amount of DGA-MWCNTs from 0.001 to 0.01 g.

Adsorption experiments were carried out at various temperature between 298 and 353 K for determining the thermodynamic parameters such as standard enthalpy change (ΔH°), entropy change (ΔS°) and free energy change (ΔG°).

Result and discussion

Characterization of functionalized CNTs

FT-IR spectroscopy

Stepwise chemical modification of MWCNTs to diglycolamide functionalized MWCNTs were monitored by analyzing the FT-IR spectra of end product at each step. FT-IR spectrum of MWCNTs (as received), carboxylated MWCNTs and diglycolamide functionalized MWCNTs are shown in Fig. 1a–c. Infrared spectra of MWCNTs (as-received) are featureless (Fig. 1a). In Fig. 1b, the peaks at $2,800\text{--}3,050 \text{ cm}^{-1}$ region are characteristic of C–H stretches and the broad shoulder band at $3,100\text{--}3,600 \text{ cm}^{-1}$ region is characteristic of acid O–H stretches. The dominant peak at $1,638 \text{ cm}^{-1}$ can be clearly assigned to the hydrogen bonded carboxylic acid and $1,448 \text{ cm}^{-1}$ peak can be due to O–H in plane bending of carboxylic acid. In the

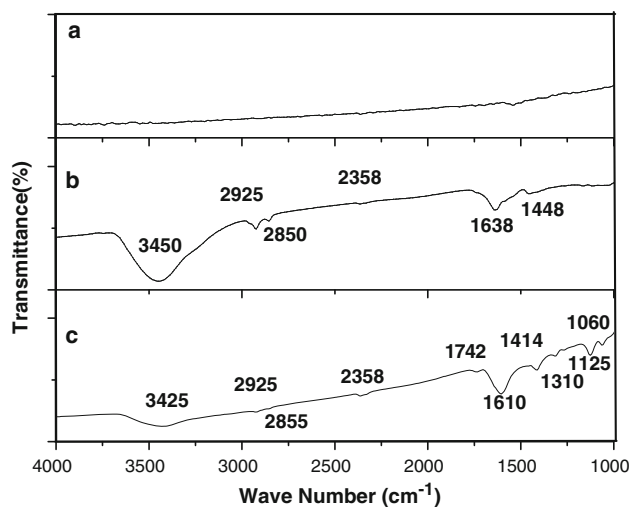


Fig. 1 FT-IR Spectra of *a* MWCNTs (as received) *b* carboxylated MWCNTs and *c* DGA functionalized MWCNTs

FT-IR spectrum of DGA-MWCNTs (Fig. 1c) the broad peak at $3,425\text{ cm}^{-1}$ can be assigned to the N–H stretching mode of the amide moiety. The peak at $1,742\text{ cm}^{-1}$ can be due to C=O stretch of acid and the peak at $1,610\text{ cm}^{-1}$ can be C=O stretch in amide moiety. Bands at $1,414$ and $1,310\text{ cm}^{-1}$ can be identified as the C–N stretching. Peaks at $1,125$ and $1,060\text{ cm}^{-1}$ are due to C–O–C stretching mode of diglycol amide group.

XRD analysis

Figure 2 shows XRD pattern of MWCNTs (as-received) and diglycolamide functionalized MWCNTs. The presence of (002) peak ($2\theta = 26.4^\circ$) in the XRD data suggests multiwalled nature of CNTs [38]. The XRD of DGA functionalized MWCNTs are very similar to that of MWCNTs (as-received). This clearly indicates that even after the functionalization there is no change in the cylindrical wall structure as raw MWCNTs and inter planar spacing [39].

SEM analysis

Figure 3 depicts the SEM image of MWCNTs (as-received) and DGA-functionalized-MWCNTs. It is observed that the tubular structure of multi-walled CNTs is well retained after functionalization.

Adsorption studies

Effect of nitric acid concentration

Studies on effect of nitric acid concentration on adsorption of uranium in DGA-MWCNTs show that the percentage of

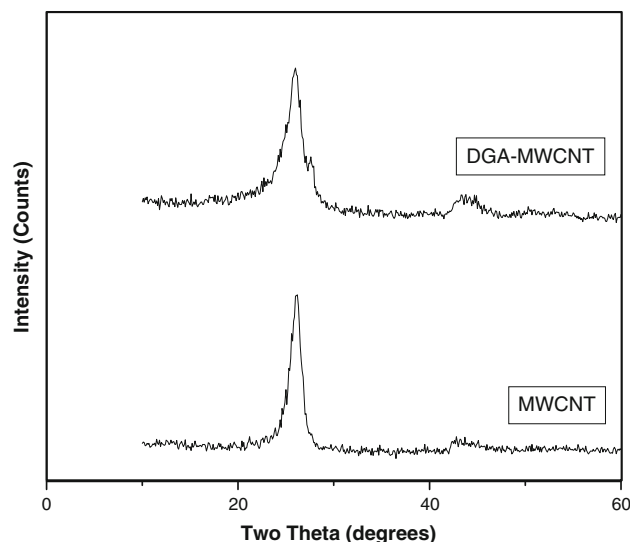


Fig. 2 XRD pattern of MWCNTs (as-received) and DGA-functionalized MWCNTs

adsorption of uranium increases sharply with acid concentration up to 4 M beyond which saturation in adsorption occurs. Figure 4 shows the variation of percentage adsorption and distribution coefficient (K_d) values for uranium as a function of nitric acid concentration. It is also observed that K_d value is increasing with increasing nitric acid concentration. At 4 M nitric acid concentration, the K_d value is $4.75 \times 10^4\text{ mL g}^{-1}$ which is about 10^2 times greater than that of various DGA modified substrates such as chromosorb-W [34], impregnated magnetic particles [40] and Amberchrom CG-71C [41]. This enhancement in K_d value can be the consequences of unique nanostructures on multiwalled CNTs.

Effect of initial uranium concentration

It was observed that adsorption of uranium is highly concentration dependent. Figure 5 shows the variation of percentage adsorption and K_d with initial uranium concentration. The percentage adsorption or K_d value increases with uranium concentration and reaches a maximum at the uranium concentration 10 mg/L and then decreases with increasing uranium concentration. In view of this, 5 mg of DGA-MWCNTs were used in these experiments.

Effect of DGA-MWCNT dose

The dependence of uranium adsorption on the amount of adsorbent, DGA-MWCNTs, is given in Fig. 6. The percentage adsorption increased sharply with increasing amount of adsorbent up to 0.005 g beyond that saturation was observed.

Fig. 3 SEM image of MWCNTs (as-received) and DGA functionalized MWCNTs

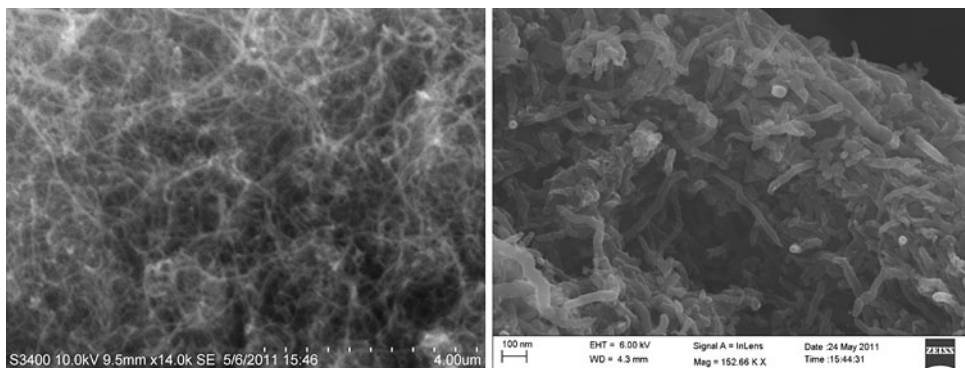


Fig. 4 Effect of nitric acid concentration on adsorption of uranium in DGA-MWCNTs

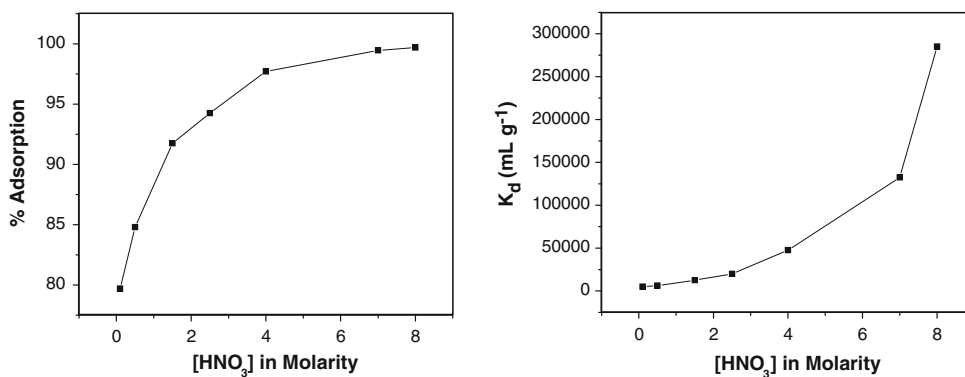
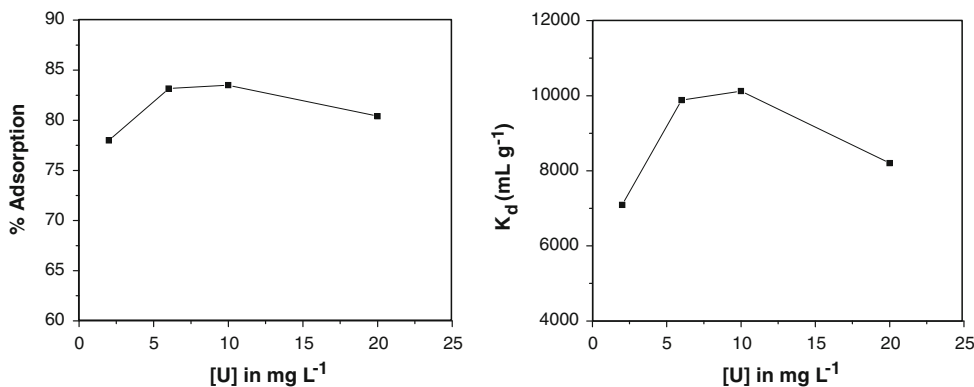


Fig. 5 Effect of uranium concentration on adsorption in DGA-MWCNTs



Adsorption isotherm

The experimental data of uranium adsorption on DGA-MWCNTs were analyzed with Langmuir and Freundlich models [30]. The adsorption isotherm plotted against experimental data is shown in Fig. 7. The equation of Langmuir and Freundlich adsorption models are expressed respectively in Eq. 3, 4.

$$\frac{C_e}{q_e} = \frac{C_e}{q_o} + \frac{1}{q_o b} \tag{3}$$

$$\ln q_e = \ln K + \frac{1}{n} \ln C_e \tag{4}$$

where C_e (mg L⁻¹) is the concentration of uranium at equilibrium and q_e (mg g⁻¹) is the amount of uranium adsorbed at equilibrium. q_e can be estimated from:

$$q_e = (C_o - C_e) \times \frac{V}{m} \tag{5}$$

C_o is the concentration of uranium in initial solution b, K and n are isotherm constants.

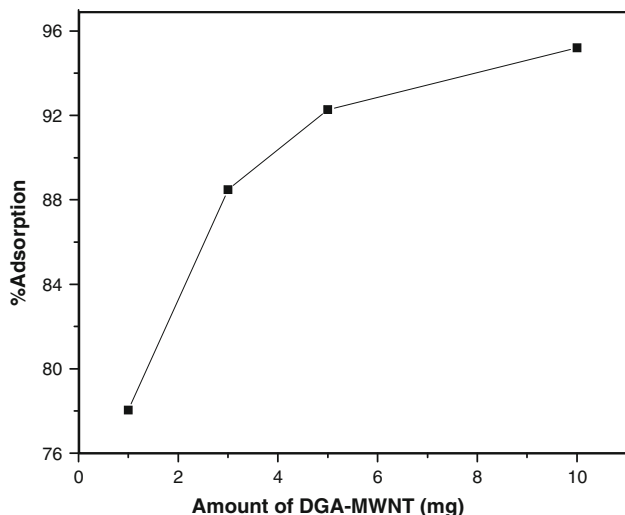


Fig. 6 Dependence of uranium adsorption on the amount of DGA-MWCNTs

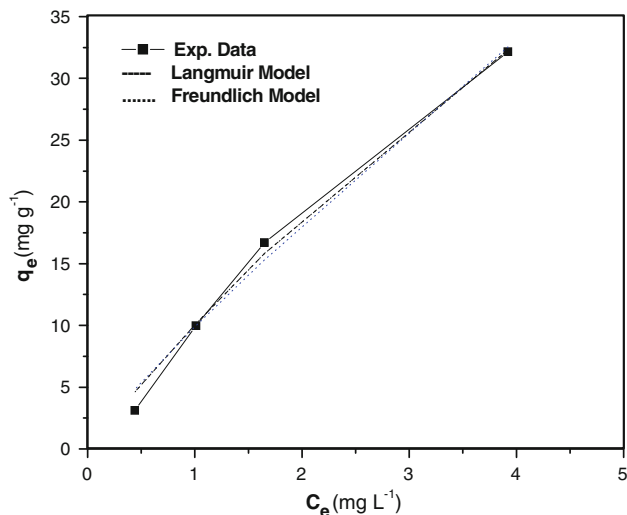


Fig. 7 The Langmuir and Freundlich isotherms plotted against experimental data of uranium adsorption in DGA-MWCNT

The value of q_0 and K can be correlated to the adsorption capacity of an adsorbent under particular experimental conditions. Linear Langmuir (C_e/q_e vs. C_e) and Linear Freundlich ($\ln q_e$ vs. $\ln C_e$) plots are used to evaluate the Langmuir and Freundlich constants tabulated in Table 2. It was observed that the Langmuir model fits the adsorption data better than the Freundlich model.

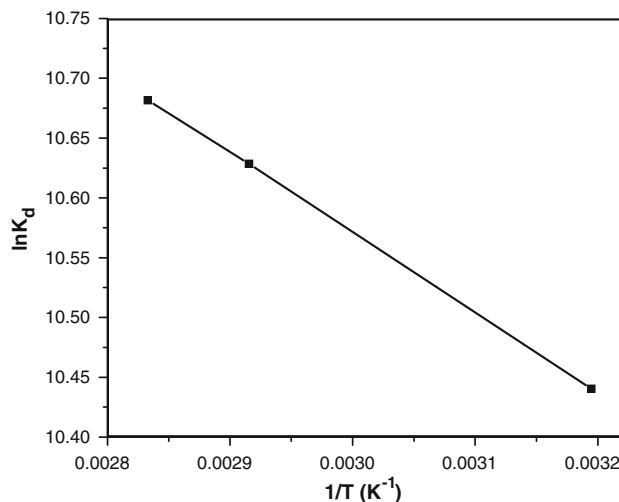


Fig. 8 Plot of Van't Hoff equation for the adsorption of uranium onto DGA-MWCNT

Adsorption thermodynamics

The thermodynamic parameters such as ΔH° and ΔS° were calculated from the slopes and intercepts of the linear regression of $\ln K_d$ versus $1/T$ plot (Fig. 8) using the Van't Hoff equation:

$$\ln K_d = \frac{\Delta S^\circ}{R} - \frac{\Delta H^\circ}{RT} \tag{6}$$

The standard free energy values were calculated from:

$$\Delta G^\circ = \Delta H^\circ - T\Delta S^\circ \tag{7}$$

The values of ΔH° , ΔS° and ΔG° are reported in Table 3. The positive value of ΔH° confirms that this adsorption of uranium on DGA-MWCNT is endothermic. The standard free energy change (ΔG°) values are negative at all temperature and decreases with increasing temperature. This indicates the spontaneous nature and feasibility of uranium adsorption on DGA-MWCNTs which becomes more favorable with increasing temperature. The positive values of entropy (ΔS°) show the increased randomness at the solid/solution interface during the adsorption process. The positive entropy of adsorption reflects the affinity of the adsorbent for uranium. The positive enthalpy change opposes the uranium adsorption but the larger entropy allows the reaction.

Table 2 Langmuir and Freundlich parameters for uranium adsorption onto DGA-MWCNTs

Langmuir constants			Freundlich constants		
q_0 (mg g ⁻¹)	b (L mg ⁻¹)	R^2	K (mg ^{1-1/n} L ^{1/n} g ⁻¹)	$1/n$	R^2
133.74	12.3	0.99	10.11	0.88	0.987

Table 3 Thermodynamic parameter for uranium adsorption on DGA-MWCNTs

ΔH° (kJ mol ⁻¹)	ΔS° (kJ mol ⁻¹ K ⁻¹)	ΔG° (kJ mol ⁻¹)				
		298 K	313 K	323 K	343 K	353 K
6.09	0.106	-25.51	-27.09	-28.16	-30.28	-31.34

Conclusions

Diglycolamide functionalized multi-walled CNTs is highly promising agent for the separation of uranium from aqueous solution with K_d value as high as 4×10^4 mL g⁻¹ at 4 M HNO₃ and at room temperature. Adsorption of uranium in DGA-MWCNTs is highly dependent on the acid concentration of solution. The percentage adsorption and K_d values depend on the initial concentration of uranium. Adsorption is favoured at higher adsorbent concentration and higher temperature. The Langmuir and Freundlich models were used for the mathematical description of the adsorption equilibrium of uranium on to DGA-MWCNTs and results show that the adsorption equilibrium data is well fitted to the Langmuir model. The temperature dependence of adsorption of uranium was investigated and thermodynamic parameters ΔH° , ΔS° and ΔG° were evaluated. The results show that the adsorption process is endothermic and the percentage of adsorption increases with increasing temperature.

Acknowledgments The authors sincerely thank Shri S.-C. Chetal, Director, IGCAR for his constant encouragements during this work. The authors thank Dr. K. Sivasubramanian, Dr. M.T. Jose, Smt. O. Annalaxmi and Ms. Anisha, Shri H. Krishnan, Shri B.-N. Mohanty, Shri Shailesh Joshi, RSD, IGCAR for their help during the experiments and analysis. The authors also thank Dr. M. Kamuruddin, SND, MSG for SEM analysis, Shri R.M. Sarguna, CMPD, MSG for XRD analysis and Shri Ajay Rawat, RSD, IGCAR for isotherm modeling.

References

- Iijima S (1991) *Nature* 354:56–58
- Long RQ, Yang RT (2001) *J Am Chem Soc* 123:2058–2059
- Liao Q, Sun J, Gao L (2008) *Colloids Surf A Physicochem Eng Aspects* 312:160–165
- Goering J, Burghus U (2007) *Chem Phys Lett* 447:121–126
- Yang K, Xing B (2009) *Environ Pollut* 157:1095–1100
- Lu C, Chung YL, Chang KF (2005) *Water Res* 39:1183–1189
- Ma X, Anand D, Zhang X, Talapatra S (2011) *J Phys Chem C* 115(11):4552–4557
- Lin D, Xing B (2008) *Environ Sci Technol* 42(19):7254–7259
- Ghaedi M, Hassanzadeh A, Nasiri Kokhdan S (2011) *J Chem Eng Data* 56(5):2511–2520
- Ramos MA, Borges JH, Miquel TMB, Delgado MAR (2009) *Anal Chim Acta* 647:167–176
- Li YH, Ding J, Luan Z, Di Z, Zhu Y, Xu C, Wu D, Wei B (2003) *Carbon* 41:2787–2792
- Li H, Pan L, Zhang Y, Sun Z (2009) *Water Sci Technol* 59.8:1657–1663
- Lu C, Chiu H (2006) *Chem Eng Sci* 61:1138–1145
- Lu C, Liu C (2006) *J Chem Technol Biotechnol* 81:1932–1940
- Hu J, Chen C, Zhu X, Wang X (2009) *J Hazard Mat* 162:1542–1550
- Stafiej A, Pyrzynska K (2007) *Sep Purifi Technol* 58:49–52
- Chen C, Hu J, Shao D, Li J, Wang X (2009) *J Hazard Mat* 164:923–928
- Ding Q, Liang P, Song F, Xiang A (2006) *Sep Sci Technol* 41:2723–2732
- Upadhyayula VKK, Deng S, Mitchell MC, Smith GB (2009) *Sci Total Environ* 408:1–13
- Chen CL, Li XL, Wang XK (2007) *Radiochim Acta* 95:261–266
- Tan XL, Chen CL, Wang XK, Hu WP (2008) *Radiochim Acta* 96:23–29
- Wang X, Chen C, Hu W, Ding A, Xu D, Zhou X (2005) *Environ Sci Technol* 39:2856–2860
- Schierz A, Zanker H (2009) *Environ Pollut* 157:1088–1094
- Perevalov SA, Molochnikova NP (2009) *J Radioanal Nucl Chem* 281:603–608
- Zhang Y, Bai Y, Yan B (2010) *Drug Discov Today* 15(11/12):428–435
- Hauke F, Hirsch A (2010) Covalent Functionalization of Carbon Nanotubes. In: Guldi DM, Martín N (eds) *Carbon nanotubes and related structures: synthesis, characterization, functionalization, and applications*. Wiley-VCH Verlag GmbH & Co. KGaA, Weinheim
- Lu C, Chiu H (2008) *Chem Eng J* 139:462–468
- Mishra AK, Arockiadoss T, Ramaprabhu S (2010) *Chem Eng J* 162:1026–1034
- Liu Y, Wu ZQ, Yan XP (2009) *Talanta* 79:1464–1471
- Afzali D, Mostafavi A (2008) *Anal Sci* 24:1135–1139
- Gupta KK, Manchanda VK, Subramanian MS, Singh RK (2000) *Sol Extr Ion Exch* 1:273–292
- Sasaki Y, Choppin GR (1996) *Anal Sci* 12:225–230
- Sharma JN, Ruhela R, Harindaran KN, Mishra SL, Tangri SK, Suri AK (2008) *J Radioanal Nucl Chem* 278(1):173–177
- Ansari SA, Pathak PN, Husain M, Prasad AK, Parmar VS, Manchanda VK (2006) *Talanta* 68:1273–1280
- Ansari SA, Mohapatra PK, Prabhu DR, Manchanda VK (2007) *J Membr Sci* 298:169–174
- Horwitz EP, McAlister DR, Bond AH, Barrans RE (2005) *Solvent Extr Ion Exch* 23:319–344
- Dialo MS, Arasho W, Johnson JH, Goddard WA (2008) *Environ Sci Technol* 42:1279–1572
- Mahanandia P, Vishwakarma PN, Nanda KK, Prasad V, Subramanyam SV, Dev SK, Satyam PV (2006) *Mater Res Bull* 41:2311–2317
- Shen J, Huang W, Wu L, Hu Y, Ye M (2007) *Mater Sci Eng A* 464:151–156
- Shaibu SS, Reddy MLP, Murali MS, Manchanda VK (2007) *Radiochim Acta* 95:159–164
- Van Hecke K, Modolo G (2004) *J Radioanal Nucl Chem* 261:269–275